Convolutional Modeling and Antenna De-embedding for Wideband Spatial mmWave Channel Measurement

Xiaofeng Lu[1], Ruonan Zhang[2], Yuliang Zhou[2], Jiawei Liu[2], Xin Jin[2], Qi Guo[2], and Chang Cao[1]
[1]Communication Technologies Laboratory, Huawei Technologies Ltd., Chengdu, China
[2]Communication Engineering Department, Northwestern Polytechnical University, Xi'an, Shaanxi, China
Emails: stan.lu@huawei.com, rzhang@nwpu.edu.cn

***Abstract*—Utilization of millimeter wave (mmWave) frequencies in the 5G has driven great efforts on measurement and modeling of the propagation channels, which are critical for the system evaluation and deployment. To compensate the large path loss, rotational scanning using high-gain horn antennas is usually employed for spatial channel characterization. However, it is a challenging issue to de-embed the antenna effect from captured channel profiles, especially for the wideband sounding. In this paper, a new convolutional modeling approach is first proposed, by which a synthesized spatial channel response is expressed by the consecutive convolutions of an antenna-free propagation model and directional antenna patterns. Then, based on the convolutional model, a simple two-step antenna de-embedding algorithm is designed. Furthermore, an indoor measurement campaign was performed using a steering receiver antenna and frequency-sweeping from 72.5 to 73.5 GHz. The high similarity between the measured and reproduced spatial channel responses and multipath impulse responses has indicated that the proposed approach can effectively de-embed the antenna effect and mitigate the system noise. It is also illustrated that the sparse impulse propagation model composed of only a few significant paths can sufficiently describe an mmWave channel. The channel angular, frequency, and time responses can be conveniently reproduced by the convolution of antenna patterns and sparse propagation models.**

I. Introduction

The bandwidth shortage has become a huge challenge for wireless service providers and motivated utilization of the millimeter-wave (mmWave) frequency spectrum in the 5G. The mmWave propagation models are critical for the design of suitable antennas and system components in typical deployment scenarios to achieve desired data rate and coverage. To understand the propagation path loss, small-scale fading, and spatial characteristics of the mmWave channels, extensive field measurements and accurate multipath parametrization are needed.

In the mmWave measurement campaigns, omni-directional antennas are limited by propagation distances (typically < 20 m) due to the large path loss. They are also difficult to provide high angular-resolution unless large antenna arrays are adopted [1]. Directional antennas, such as steerable horn antennas, have been widely adopted to compensate the path loss by high antenna gains [2], [3]. Meanwhile, since a horn antenna has limited half power beam width (HPBW), the angular-domain information can be acquired with spatial scanning by rotating the antenna. The spatial parameters of propagation paths, such as the angle-of-arrival (AoA), angle-of-departure (AoD), and angular power spectra, can be obtained. The approach offers substantial improvement in measurement range compared to using omni-directional low-gain antennas. However, antenna patterns are embedded in the captured channel profiles and become a part of the radio channel responses under measurement. In order to achieve antenna-free channel characteristics, the antenna effect need to be de-embedded from the captured channel responses. Then the obtained general channel models can be used in system simulations, where synthesized channel models are constructed with the antenna patterns of practical systems. Therefore, to de-embed the antenna effect in field measurements is a critical issue in the mmWave channel measurements using high-gain horn antennas and antenna-steering solution.

The authors in [4] proposed a method of summing up the received power from every measured non-overlapping angular range, and the omni-directional antenna pattern and received power were synthesized from the measured data by the angular combination. An approach to extract the narrowband propagation channel description from a communication link by de-embedding the impact of antennas was proposed in [5]. A propagation channel in the spherical vector wave domain was expressed by a mode-to-mode mapping matrix, and was estimated by applying pseudo-inverse computation to the channel transfer functions. In [6], the authors proposed a method to de-embed antennas from a single channel sounding measurement using high-resolution multipath AoA/AoD estimations. Different antennas could be efficiently described and interpolated by the effective aperture distribution function (EADF) and thus evaluated without re-running measurement campaigns. In [7], the authors proposed a simple de-convolution algorithm for antenna de-embedding. The method was validated by demonstrating that the synthesized omni-directional channel responses were independent of antenna beamwidth, through mmWave propagation measurements using antennas with different beamwidths.

The wideband channel sounding to characterize the frequency-selective fading is important for mmWave channel modeling, to support the design of extremely-high-speed communications. Since the channel is measured in both the frequency and space domains using steering horn antennas, the antenna de-embedding should be performed jointly in the

978-1-5090-4183-1/17/$31.00 ©2017 IEEE

two domains. Therefore, it is more challenging for the spatial channel responses over a large frequency bandwith. The works mentioned above mainly studied the narrow-band channel sounding and signal processing technologies. The wideband joint frequency-space domain signal modeling and antenna de-embedding approach is needed and has not been explored.

In this paper, the wideband signal model and antenna de-embedding algorithm for mmWave channel measurement using steerable horn antennas are proposed. The main contributions are two-fold.

First, a new convolutional signal model for wideband mmWave channel responses using steering horn antennas is proposed. The synthesized frequency-space channel response is expressed in a term of consecutive convolutions of the antenna-free propagation model, pattern of the steering transmitter (Tx) antenna, and pattern of the steering receiver (Rx) antenna. This modeling approach is the basis for the following antenna de-embedding operation. Also, by using this convolutional model, the synthesized channel responses for different antenna types under various propagation conditions can be recreated without re-running measurement campaigns.

Second, a simple two-step antenna de-embedding algorithm is designed for the wideband antenna-steering mmWave channel measurement data. At first, the directions of the significant paths are estimated by de-convolution of the antenna patterns. Then the antenna patterns are sampled at the potential directions of the paths, and the path gains are determined by using the inverse of the selected antenna responses.

Furthermore, to validate the proposed approach, a field measurement campaign was performed on the wideband spatial mmWave channel in an office. The measurement was conducted using a steering horn antenna with a 20 dB gain at the Rx and the frequency-sweeping technology. The channel was sounded using a single-tone signal whose frequency incremented from 72.5 to 73.5 GHz with a 1 MHz step. The frequency-space channel responses with the antenna pattern embedded were obtained. By using the proposed approach, the antenna-free frequency-space propagation model is obtained. Then the angular responses, transfer functions, and channel impulse responses (CIRs) for a given direction and omni-direction are reproduced by using the estimated propagation model. The high similarity between the reproduced and measured responses has verified that the proposed approach can effectively de-embed the antenna effect and also mitigate the noise in the measurement.

In addition, it is observed that the channel responses reproduced by using the convolution of the antenna pattern and *sparse impulse model* composed of several significant paths can achieve high similarity with the measured results. Including more paths in the propagation model will not increase the fidelity much. Therefore, the sparse impulse propagation model can sufficiently describe the mmWave channels and the channel responses in the space, frequency, and time domains can be synthesized by the convolution of the model and antenna patterns.

The proposed approach including the sparse convolutional signal model and the antenna de-embedding algorithm provides a tool to extract the antenna-free propagation model from channel sounding data and perform channel synthesis. Compared to the traditional stochastic scattering models, the approach is more realistic because it does not rely on simplified/compressed channel parametrization from statistical distribution functions. By using the method, the channel responses for different prototype antennas under various propagation conditions can be produced without re-running measurement campaigns.

The rest of the paper is organized as follows. In Sec. II, the convolutional model of the frequency-space channel response in the wideband spatial mmWave channel measurement is defined. The antenna pattern de-embedding algorithm is proposed in Sec. III. In Sec. IV, the field mmWave channel measurement campaign is described and the antenna de-embedding results are presented, and the sparse impulse model for the mmWave channels is illustrated. Sec. V concludes the paper and points out the future research issues.

II. Convolutional Channel Model

A. Signal Model for Frequency-Space Channel Response

Suppose that there are L propagation paths and their complex gains at the frequency f are $h_l(f) = \alpha_l(f)e^{j\theta_l(f)}$ where $\alpha_l(f)$ and $\theta_l(f)$ are the magnitude and phase shift of the l-th path ($l = 1, 2, \cdots, L$), respectively. The AoDs and AoAs of the paths are $\phi_{d,l}$ and $\phi_{a,l}$, respectively. The frequency-space channel model can be expressed as

$$h(f, \phi_t, \phi_r) = \sum_{l=1}^{L} h_l(f)\, \delta(\phi_t - \phi_{d,l})\, \delta(\phi_r - \phi_{a,l}), \quad (1)$$

where ϕ_t and ϕ_r are the azimuth and elevation angles with respect to the Tx and Rx antennas, respectively. In (1), the traditional "clustering" of paths is not included because, as shown in the following sections, the mmWave channels can be described and the synthetic responses can be reproduced by several sparse significant paths.

Channel sounding using steering horn antennas combined with frequency sweeping is illustrated in Fig. 1. The Tx antenna is rotated to M angles over the range of $[-\pi,\ \pi]$, denoted by $\phi_{t,m}$ where $m = 1, 2, \cdots, M$. Meanwhile, the Rx antenna is rotated to N angles, $\phi_{r,n}$ where $n = 1, 2, \cdots, N$ from $-\pi$ to π. When the Tx antenna and the Rx antenna are rotated to certain angles, a complex channel response (a scale value) can be observed.

The complex patterns of the Tx and Rx antennas are denoted by $a_t^*(f, \phi_t)$ and $a_r^*(f, \phi_r)$, respectively, which are measured in an anechoic chamber. The antenna patterns are sampled at the rotation angles and expressed as

$$\begin{cases} a_t(f, \phi_t) = \sum_{m=1}^{M} a_t^*(f, \phi_{t,m})\, \delta(\phi_t - \phi_{t,m}), \\ a_r(f, \phi_r) = \sum_{n=1}^{N} a_r^*(f, \phi_{r,n})\, \delta(\phi_r - \phi_{r,n}). \end{cases} \quad (2)$$

When the Tx antenna is pointing to the angle of $\phi_{t,m}$ and transmitting the single-tone signal at the frequency f, if the signal is effectively radiated from the AoDs of $\phi_{d,l}$,

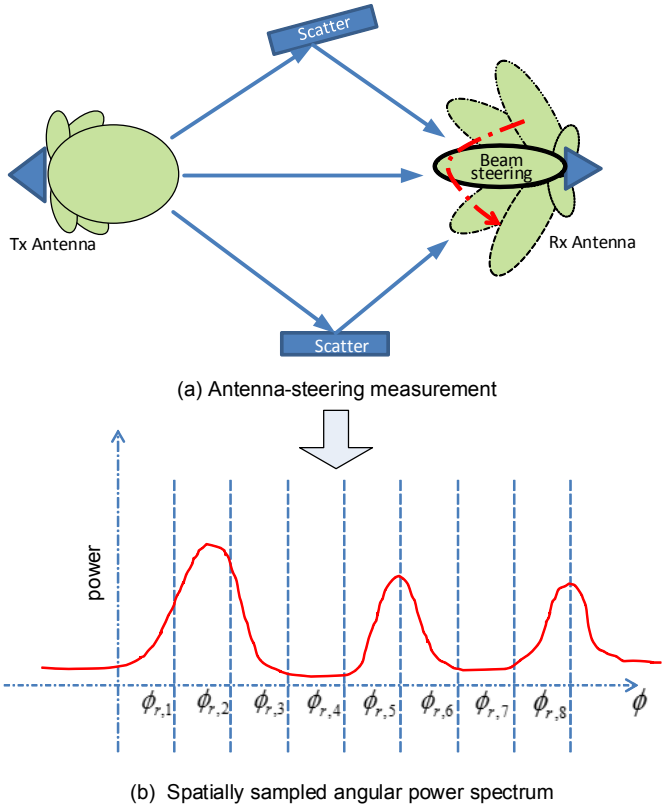

Fig. 1. Spatial channel sampling using steering directional antennas.

it is weighted by the Tx antenna pattern at these angles. On the Rx side, when the Rx antenna is pointing to the angle of $\phi_{r,n}$, the received signal is actually the superposition of the impinging waves at the AoAs of $\phi_{a,l}$ attenuated by the antenna gains at these directions. Therefore, the synthesized frequency-space channel response can be regarded as the convolution of the spatial propagation path gains, Tx antenna pattern, and Rx antenna pattern. Thus, the wideband spatial convolutional signal model (*i.e.*, the observed frequency-space channel response) for the antenna-steering mmWave channel measurement is expressed as

$$y(f,\phi_t,\phi_r) = h(f,\phi_t,\phi_r) \otimes a_t(f,\phi_t) \otimes a_r(f,\phi_r), \quad (3)$$

where f is the frequency of the probing signal, $a_t(f,\phi_t)$ and $a_r(f,\phi_r)$ are the sampled antenna patterns given in (2). Our object is to obtain the estimate of the antenna-independent channel model in the frequency-space domain, $\hat{h}_l(f,\phi_t,\phi_r)$ as defined in (1). Different from the traditional channel models, (3) separates the propagation model and antenna patterns in the form of consecutive convolutions, which can help to de-embed the antenna impact and also reconstruct the synthetic channel responses, as discussed in the next section.

If an omni-directional Tx antenna is employed in the channel measurement campaign, (3) can be simplified as

$$y_r(f,\phi_r) = a_t^o(f)\left\{\sum_{l=1}^{L} h_l(f)\,\delta(\phi_r - \phi_{a,l})\right\} \otimes a_r(f,\phi_r), \quad (4)$$

where $a_t^o(f)$ is the omni-directional gain of the Tx antenna. In this case, the parameter set is

$$\Omega_p = \{L, h_l, \phi_{a,l}\}, \qquad \text{for} \quad l = 1,2,\cdots,L \quad (5)$$

which needs to be estimated.

B. Channel Model Estimation

Estimation of the path parameter set Ω_p from the observed data can be obtained by the maximum-likelihood (ML) method. Let $\hat{\Omega}_p = \left\{\hat{L}, \hat{h}_l, \hat{\phi}_{a,l}\right\}$ denote the estimate of the parameters. Based on (4), the object function to de-embed the Rx antenna pattern can be derived as

$$\arg\min_{\hat{\Omega}_p} \left| \begin{array}{l} \frac{1}{a_t^o(f)} \sum_{l=1}^{\hat{L}} \hat{h}_l(f)\,\delta\left(\phi_r - \hat{\phi}_{a,l}\right) \\ \otimes a_r(f,\phi_r) - y_r(f,\phi_r) \end{array} \right|, \quad (6)$$

where the synthetic channel response is reconstructed by the convolution of the propagation model and Rx antenna pattern and approaches the received signals (observation). However, to solve the optimization problem in (6) requires exhaustive multi-dimensional searching over the parameter set, and the computational complexity is prohibitively high. Although the expectation maximization (EM) and SAGE algorithms can reduce the complexity significantly by iterative searching on subsets of the parameters, large computational resource and time are still required.

On the other hand, based on (4), the channel model estimate, $\hat{h}_l(f,\phi_r)$, can be obtained directly by de-convolution. But (4) is an ill-posed inversion problem due to the noise in the received signals. It is non-trivial to mitigate the noise and identify the propagation paths.

III. Antenna De-Embedding and Propagation Modeling

A. Antenna De-Embedding Algorithm

In this section, we propose a simple antenna de-embedding algorithm for the frequency-space mmWave channel measurement. For easy presentation, the algorithm is given as following based on the simplified signal model in (4) where an omni-directional Tx antenna is adopt. The extension of the method for using directional antennas at both ends as given in (3) will be addressed in our future works. Suppose that an mmWave channel is measured at a total of K carrier frequencies (f_k for $k = 1,2,\cdots,K$) by discrete frequency-sweeping and the Rx antenna is rotated to N directions at the angles of $\phi_{r,n}$ for $n = 1,2,\cdots,N$. For each frequency and direction, a complex channel response value is recorded.

Step 1: The received spatial responses over the N angles at the frequency of f_k are organized in a vector of

$$\mathbf{y}_k = \begin{bmatrix} y_{k,1} & y_{k,2} & \cdots & y_{k,N} \end{bmatrix}^{\mathrm{T}}, \quad (7)$$

where $y_{k,n}$ is the observed complex response when the Rx antenna is pointing to the direction of $\phi_{r,n}$ and $[\cdot]^{\mathrm{T}}$ represents the matrix transport. $y_{k,n}$ are actually the samples of $y_r(f, \phi_r)$ given in (4), by spatially sampling the channel response at the Rx antenna rotation angles in the azimuth (or elevation) domain.

Step 2: Generate the angularly discretized Rx antenna pattern sampled at the rotation angles $\phi_{r,n}$, which is

$$\mathbf{a}_k = \begin{bmatrix} a_r\left(f_k, \phi_{r,1}\right) & a_r\left(f_k, \phi_{r,2}\right) & \cdots & a_r\left(f_k, \phi_{r,N}\right) \end{bmatrix}^{\mathrm{T}}. \tag{8}$$

Furthermore, the discrete antenna pattern circularly is shifted to the angle of $\phi_{r,n}$ ($n = 1, 2, \cdots, N$), which is denoted by $\mathbf{a}_{k,n}$ and defined as

$$\begin{aligned} \mathbf{a}_{k,n} = \begin{bmatrix} a_r\left(f_k, \phi_{r,n}\right) & a_r\left(f_k, \phi_{r,n+1}\right) & \cdots & a_r\left(f_k, \phi_{r,N}\right) \\ a_r\left(f_k, \phi_{r,1}\right) & a_r\left(f_k, \phi_{r,2}\right) & \cdots & a_r\left(f_k, \phi_{r,n-1}\right) \end{bmatrix}^{\mathrm{T}}. \end{aligned} \tag{9}$$

Step 3: Construct the convolution matrix of the discretized antenna pattern, which is expressed by

$$\mathbf{A}_k = \begin{bmatrix} \mathbf{a}_{k,1} & \mathbf{a}_{k,2} & \cdots & \mathbf{a}_{k,N} \end{bmatrix}^{\mathrm{T}}. \tag{10}$$

Perform the space-domain de-convolution by multiplying the inverse of the convolution matrix with the measurement data. Thus, the gross spatial spectrum (GSS), denoted by $\mathbf{s}_k$, is obtained as

$$\mathbf{s}_k = \mathbf{A}_k^{-1} \mathbf{y}_k. \tag{11}$$

The obtained spectrum $\mathbf{s}_k$ cannot provide the accurate estimate of the complex response of the propagation paths due to the noise, but it can indicate the incident directions of the paths.

Step 4: Pick out the local maxima of $\mathbf{s}_k$ and collect their directions. Please note that, since the antenna main lobe has a certain beam width, the noise may generate local peaks randomly around the spectrum peaks pointing to the propagation paths. Therefore, the selected peaks should be angularly spaced larger than the beam width to avoid the false paths. Suppose that we select L paths with the largest power by searching for the local peaks. Their directions are ϕ_{r,n_l} for $l = 1, 2, \cdots, L$. Please note we can select different numbers of paths L, which determines the fidelity of the channel model and the final synthesized responses. The larger L is, the more fidelity they will be. The similarity between the measured and synthesized channel responses using different numbers of paths will be compared in the next section.

For each incident direction of the paths ϕ_{r,n_l}, we can "virtually" point the antenna to the direction by circularly shifting the antenna pattern vector $\mathbf{a}_k$ by n_l, *i.e.*, $\mathbf{a}_{k,n_l}$ as defined in (9). Thus, a total of L shifted antenna patterns are obtained and organized in a $N \times L$ matrix of

$$\mathbf{A}_{k,L} = \begin{bmatrix} \mathbf{a}_{k,n_1} & \mathbf{a}_{k,n_2} & \cdots & \mathbf{a}_{k,n_L} \end{bmatrix}, \tag{12}$$

and $\mathbf{A}_{k,L}$ is called the *selected antenna pattern matrix (SAPM)*.

Step 5: The complex gains of the L paths for the frequency f_k, denoted by $h_{k,l}$ for $l = 1, 2, \cdots, L$, is calculated by

$$\begin{bmatrix} \hat{h}_{k,1} & \hat{h}_{k,2} & \cdots & \hat{h}_{k,L} \end{bmatrix}^{\mathrm{T}} = \left(\mathbf{A}_{k,L}^{\mathrm{T}} \mathbf{A}_{k,L}\right)^{-1} \mathbf{A}_{k,L}^{\mathrm{T}} \mathbf{y}_k, \tag{13}$$

where $\mathbf{A}_{k,L}$ is given in (12).

Finally, the *omni-directional spatial channel model* estimation for the frequency f_k is $\hat{\mathbf{h}}_k^{o,s} = \begin{bmatrix} x_1 & x_2 & \cdots & x_N \end{bmatrix}^{\mathrm{T}}$ where, for $i = 1, 2, \cdots, N$,

$$x_i = \begin{cases} \hat{h}_{k,l}, & \text{if } i = n_l \\ 0. & \text{otherwise} \end{cases} \tag{14}$$

By repeating Step 1 to 5 for all the probing frequencies, the frequency-space channel model can be obtained over the angular range of $[\phi_{r,1},\ \phi_{r,N}]$ and the measured frequencies of f_k ($k = 1, 2, \cdots, K$).

B. Channel Model in the Frequency and Time Domains

From the frequency-space channel model $\hat{\mathbf{h}}_k^{o,s}$, the channel response in the frequency-domain and the impulse response in the time domain for a given direction and the omni-direction can be obtained as following.

- For the directional propagation model, the complex path gains can be selected from $\hat{\mathbf{h}}_k^{o,s}$ for all measured frequencies (for $k = 1, 2, \cdots, K$) and at a given direction ($\phi_{r,n}$). They constitute the frequency response at the direction. Thus, the directional transfer function at $\phi_{r,n}$ is

  $$\hat{\mathbf{h}}_n^{d,f} = \begin{bmatrix} \hat{h}_{1,n} & \hat{h}_{2,n} & \cdots & \hat{h}_{K,n} \end{bmatrix}^{\mathrm{T}}. \tag{15}$$

  Then the wideband CIR at the direction of $\phi_{r,n}$ can be calculated by $\hat{\mathbf{h}}_n^{d,\tau} = \mathcal{F}^{-1}\left(\hat{\mathbf{h}}_n^{d,f}\right)$, where $\mathcal{F}^{-1}(\cdot)$ is the short-time inverse Fourier transform (ST-IFT) with a truncated window in the frequency domain such as the Hamming window.
- For the omni-directional propagation model, we can first sum up the path gains from all the directions at a given frequency. The composite omni-directional gain at the frequency f_k is

  $$\hat{h}_k^o = \sum_{l=1}^{L} \hat{h}_{k,l}, \tag{16}$$

  where $\hat{h}_{k,l}$ is from $\hat{\mathbf{h}}_k^{o,s}$ given in (13).
  Then the omni-directional transfer function is

  $$\hat{\mathbf{h}}^{o,f} = \begin{bmatrix} \hat{h}_1^o & \hat{h}_2^o & \cdots & \hat{h}_K^o \end{bmatrix}^{\mathrm{T}}. \tag{17}$$

  The wideband omni-directional CIR is calculated by $\hat{h}^{o,\tau} = \mathcal{F}^{-1}\left(\hat{\mathbf{h}}^{o,f}\right)$.

In addition, at a certain carrier frequency f_k, the measured spatial channel response can be reconstructed by

$$\hat{\mathbf{y}}_k = \hat{\mathbf{h}}_k^{o,s} \otimes \mathbf{a}_k. \tag{18}$$

Then $\hat{\mathbf{y}}_k$ can be compared with the observed spatial channel response, $\mathbf{y}_k$, to verify the antenna de-embedding result.

IV. Channel Measurement Campaign and Algorithm Validation

A. Measurement Setting

In order to verify the convolutional frequency-space channel modeling approach given in Sec. II and the antenna de-embedding algorithm in Sec. III, a measurement campaign on the mmWave channel from 72.5 to 73.5 GHz using a steerable horn Rx antenna was conducted in an office of the HUAWEI company, Chengdu, China. The office had the size of 56×34 m^2 and the height of 4.5 m. There were tables, chairs, pillars, whiteboard, and computers in the office. Dual-pane windows stood by one side of the office, while the other sides were dry walls of meeting rooms. The line-of-sight (LOS) scenario was measured.

The channel was sounded by using an S-parameter network analyzer, Agilent 8722ES. The heights of the Tx and Rx antennas were fixed as 2.4 and 1.5 m, respectively. An fixed Tx antenna and a steerable horn Rx antenna were employed. The HPBW and gain of the Rx antenna were 17° and 20 dBi. To measure the multipath propagation in the azimuth domain, a direction-scanning sounding scheme described in Fig. 1 was adopted. The Rx antenna was rotated from -180° to $+180^\circ$ with the angular step of 2° (thus $N = 180$) in the horizontal plane. The elevation angle of the horn antenna was always 4° because the Rx was located lower than the Tx. Meanwhile, for the frequency domain, the channel was sounded using the frequency-sweeping single-tone signal with the frequency changing from 72.5 to 73.5 GHz and 1 MHz spacing. Hence, when the Rx antenna was pointing to a direction, the channel was probed by $1,001$ times and, for every carrier frequency, a complex value of the channel response was recorded. Consequently, a complex azimuth response from -180° to $+180^\circ$ with 180 samples was observed. The environment was static without objects moving during the measurements.

B. Measurement Results and Analysis

As illustrative examples, the measured azimuth channel response $\mathbf{y}_k$, the estimated path gains $\hat{\mathbf{h}}_k^{o,s}$ given in (14), and the reproduced spatial response ($\hat{\mathbf{y}}_k$ given in (18)) in the space domain at two carrier frequencies (73 and 73.4 GHz) are plotted in Fig. 2. As can be seen, the obtained antenna-free propagation model can accurately indicate the incident directions and amplitudes of the impinging waves. The reconstructed angular responses coincide well with the measurement results. The observations verify that the proposed signal model and approach are effective in de-embedding the antenna effect and reducing the noise for the mmWave channel measurement.

We have also used different numbers of selected paths (L is increased from 1 to 10) in the antenna-free channel model ($\hat{\mathbf{h}}_k^{o,s}$) to reproduce the azimuth channel responses. The reconstructed responses by using different numbers of paths are compared with the measurement result. The correlation coefficients are listed Table IV-B and plotted in Fig. 3. Since the channel was sounded at 1,001 frequencies, the correlation results at three frequencies are listed as illustrative examples and the average results for all the frequencies are provided.

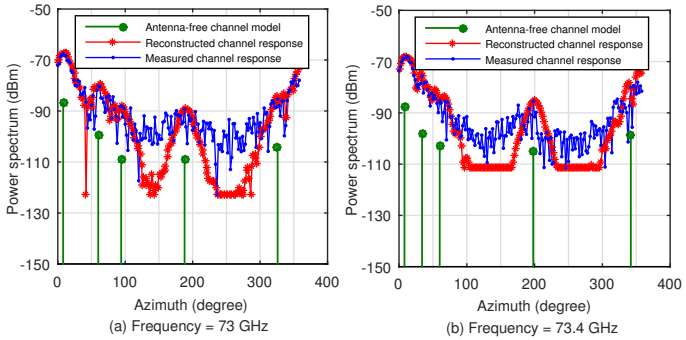

Fig. 2. Measured and reproduced azimuth channel responses and spatial propagation model at two frequencies.

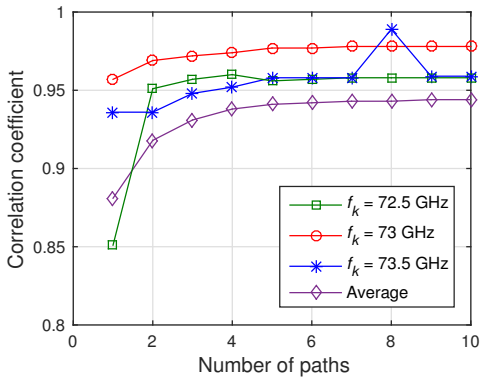

Fig. 3. Correlation coefficients between the reconstructed and measured channel responses.

First, the correlation coefficients are always larger than 0.85, which indicates that the impulse-based propagation model can reasonably reproduce the channel responses by convolution with the antenna pattern. The discrepancies between the reproduced and measured responses should be mainly caused by the noise. Second, we can see that the correlation coefficients do not increase much when L is larger than 5. This shows that 6 or more paths do not increase the fidelity of the antenna-free channel model and only 5 paths can sufficiently reconstruct the channel response by convolution. Therefore, a *sparse channel model* with only a small number of significant paths can be utilized to represent the indoor mmWave channel.

As shown in Fig. 2, the five significant paths arrived at the azimuth angles of about 12°, 56°, 116°, 206°, and 332° (the directions may change at different frequencies due to the varying propagation power). For one direction, the measured directional transfer function is obtained by organizing the observed channel response at all frequencies f_k into a vector, and then the measured directional CIR, $\mathbf{h}_n^{d,\tau}$, is acquired by ST-IFT. On the other hand, based on the five-path sparse channel model established above, we can organize the path gains at all the frequencies at one direction into a vector, *i.e.*, the directional transfer function of the channel model as given in (15). Then the directional synthesized CIR model, $\hat{\mathbf{h}}_n^{d,\tau}$, is obtained according to Sec. III-B. As illustrative

TABLE I
CORRELATION COEFFICIENTS BETWEEN THE RECONSTRUCTED AND MEASURED CHANNEL RESPONSES

No. of paths	1	2	3	4	5	6	7	8	9	10
72.5 GHz	0.851	0.951	0.957	0.960	0.956	0.957	0.958	0.958	0.958	0.958
73 GHz	0.957	0.969	0.972	0.974	0.977	0.977	0.978	0.978	0.978	0.978
73.5 GHz	0.936	0.936	0.948	0.952	0.958	0.958	0.958	0.989	0.959	0.959
Average	0.881	0.918	0.931	0.938	0.941	0.942	0.943	0.943	0.944	0.944

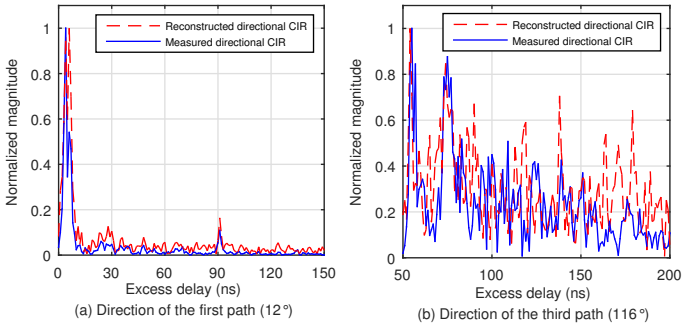

Fig. 4. Measured and reproduced directional CIRs at two directions.

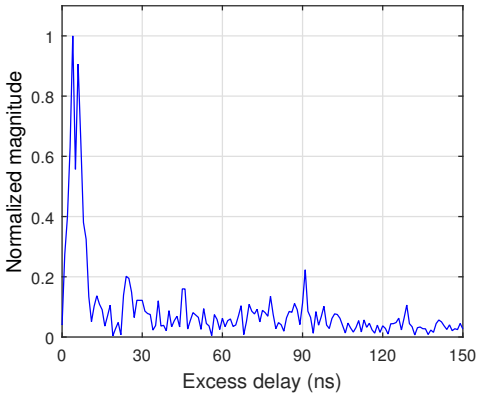

Fig. 5. Reproduced omni-directional CIR for the wideband mmWave channel.

examples, the measured and the reproduced directional CIRs at the azimuth angles of 12° and 116° are plotted in Fig. 4. We can see that they agree reasonably well with each other.

Finally, based on the established five-path frequency-space propagation model, the omni-directional wideband transfer function can be obtained as given in (17). Then the omni-directional multipath CIR, $\hat{h}^{o,\tau}$, can be calculated by ST-IFT, which is plotted in Fig. 5.

As can be observed, the measured channel responses in the space, frequency, and time domains can be reconstructed by using the antenna-free sparse propagation model as given in Sec. III-B. The comparison has verified the accuracy and feasibility of the convolutional model and the antenna de-embedding algorithm.

V. CONCLUSION

In this paper, a convolutional signal model is first proposed for the antenna-steering channel response, where the "pure" channel model and antenna patterns are separated in the form of convolutions. Then a novel antenna de-embedding and noise removing method is proposed, and its feasibility has been demonstrated by an mmWave measurement campaign using a steerable horn antenna at the Rx. Furthermore, it is shown that the sparse channel model composed of only a few significant paths can sufficiently reproduce the mmWave channel responses. This study answered important questions regarding antenna de-embedding and sparse convolutional modeling approach for mmWave channel measurement. The proposed method can help to construct an omnidirectional channel model while enhancing the measurement range substantially by using high-gain directional antennas. More accurate antenna de-embedding algorithms based on sparse mmWave channel models are interesting research topics for future works.

ACKNOWLEDGEMENT

This work was supported in part by NSFC (61571370, 61301092, and 61601365), Natural Science Basic Research Plan in Shaanxi Province (2015JM6349 and 2016JQ6017), and National Civil Aircraft Major Project of China (MIZ-2015-F-009).

REFERENCES

[1] R. Zhang, S. Wang, X. Lu, W. Duan, and L. Cai, "Two-dimensional DoA estimation for multipath propagation characterization using the array response of PN-sequences," *IEEE Trans. Wireless Commun.*, vol. 15, no. 1, pp. 341–356, Jan. 2016.

[2] M. K. Samimi, G. R. MacCartney, S. Sun, and T. S. Rappaport, "28 GHz millimeter-wave ultrawideband small-scale fading models in wireless channels," in *Proc. IEEE Vehicular Technology Conference (VTC-Spring)*, Nanjing, China, May 2016, pp. 1–6.

[3] T. S. Rappaport, F. Gutierrez, E. Ben-Dor, J. N. Murdock, Y. Qiao, and J. I. Tamir, "Broadband millimeter-wave propagation measurements and models using adaptive-beam antennas for outdoor urban cellular communications," *IEEE Trans. Antennas Propag.*, vol. 61, no. 4, pp. 1850–1859, Apr. 2013.

[4] S. Sun, G. R. MacCartney, M. K. Samimi, and T. S. Rappaport, "Synthesizing omnidirectional antenna patterns, received power and path loss from directional antennas for 5G millimeter-wave communications," in *Proc. IEEE Global Communications Conference (Globecom)*, San Diego, CA, Dec. 2015, pp. 1–7.

[5] Y. Miao, K. Haneda, M. Kim, and J. Takada, "Antenna de-embedding of radio propagation channel with truncated modes in the spherical vector wave domain," *IEEE Trans. Antennas Propag.*, vol. 63, no. 9, pp. 4100–4110, Sep. 2015.

[6] M. Kaske, C. Schneider, W. Kotterman, and R. Thoma, "Solving the problem of choosing the right MIMO measurement antenna: Embedding/de-embedding," in *Proc. European Conference on Antennas and Propagation (EuCAP)*, Rome, Italy, Apr. 2011, pp. 2551–2555.

[7] S. X. Lu, R. Zhang, C. Cao, and X. Zou, "Design and experimental validation of a simple antenna de-embedding approach for mmWave channel modeling," in *Proc. IEEE Radio and Wireless Symposium (RWS)*, Phoenix, AZ, Jan. 2017, pp. 1–4.